UNIVERSIDADE DE SÃO PAULO

INSTITUTO DE FÍSICA
CAIXA POSTAL 20516
01498 - SÃO PAULO - SP
BRASIL

PUBLICAÇÕES

IFUSP/P-863

TWO-NEUTRON REMOVAL CROSS SECTIONS OF ^{11}Li-PROJECTILES

C.A. Bertulani and G. Baur
Institut für Kernphysik, KFA, Postfach 1913
5170 Jülich, F.R.G.

M.S. Hussein
Instituto de Física, Universidade de São Paulo

Agosto/1990

TWO–NEUTRON REMOVAL CROSS SECTIONS OF ^{11}Li–PROJECTILES

C.A. Bertulani[*,**] **and G. Baur**

Institut für Kernphysik, KFA, Postfach 1913, 5170 Jülich, F.R.G.

and

M.S. Hussein[**]

Instituto de Física, Universidade de São Paulo
C.P. 20516, 01849 São Paulo, SP, Brazil

ABSTRACT

We investigate the interplay of the nuclear and Coulomb interaction in the fragmentation of relativistic ^{11}Li–projectiles incident on several targets. The ^{11}Li nucleus is assumed to have a cluster–like structure, with a (bound) di–neutron system coupled to a ^{9}Li–core in a s–state. It is shown that, while the Coulomb contribution can be fairly well described in such model, the obtained nuclear cross sections show markedly differences with the experimental data. But, since the separation of the Coulomb and the nuclear contribution is theoretical in principle, this comparison points out ambiguities in the analysis of the experimental data.

* Permanent adress: Intituto de Física, UFRJ, 21945 Rio de Janeiro, Brazil.

** Supported in part by CNPq and FAPESP.

July/1990

The fragmentation of neutron–rich nuclei has led to many unusual speculative ideas about their structure. Perhaps, the most interesting one is due to Hansen and Jonson[1], who proposed a clusterlike structure for ^{11}Li as composed by a di–neutron system loosely–bound to a ^{9}Li–core. This hypothesis has had a general support from several other authors[2–6]. It seems that such cluster structure occurs very often in light–neutron–reich nuclei and results from a delicate balance between the neutron–neutron and neutron–core interactioons[2]. The Hansen–Jonson model is supported by several facts. Firstly, the separation energy of two neutrons from ^{11}Li is very low[7–8], $S_{2n} = 250 \pm 80$ KeV. Otherwise, the nucleus ^{10}Li does not exist[9], having a resonant continuum state at 800 ± 250 KeV. This means that the neutron–neutron interaction acquires a stronger attractive character in the presence of the ^{9}Li–core. Secondly, the experimental measurements of total reaction cross sections[10] of neutron–rich nuclei incident on several targets at 0.8 GeV/nucleon reveal an *rms* radius of 3.14 ± 0.06 fm for ^{11}Li, compared to an *rms* radius of 2.41 ± 0.02 fm for ^{9}Li. A large increase of matter radius from ^{12}Be to ^{14}Be, and possibly from ^{15}B to ^{17}B, is also observed. The lasst two neutrons are responsible for the unusual increase of the matter radius and for the appearence of a "neutron–halo" in these nuclei. In the cluster model the existence of such halo can be easily explained as due to the low binding energy of the di–neutron system. In fact, by assuming a deuteron–like wavefunction for ^{11}Li and adjusting it to reproduce the binding energy of the dineutron system, an approximate *rms* mean distance of the dineutron to the core of 6 fm is obtained. This rould essentially explain the *rms* radius of ^{11}Li as roughly given by $2R_{\mathrm{m.s.}}^{(2n)}/11 + 9R_{\mathrm{m.s.}}^{(9)}/11 = 2 \times 6/11 + 2.41/11 \cong 3.1$ fm.

Another support for the cluster–model for ^{11}Li is that the experimentally determined[10] electromagnetic dissociation cross sections for ^{11}Li can be well described theoretically[1–6]. The momentum distribution of the ^{9}Li–fragments are also well fitted within this model, as was shown in ref.4. In contrast to this, conventional shell model calculations performed by Bertsch and collaborators[11–13] were not able to reproduce the

amount of electric dipole strength in ^{11}Li necessary to explain the electromagnetic dissociation cross sections. As concluded by Bertsch and Foxwell[11] it may be essential to take cluster aspects into account. The failure of the shell model calculations to determine the enhancement of the electric dipole strength of ^{11}Li at low energies – which is needed to reproduce the experimental data – has lead the authors in ref.13 to argue if experimental values of the electromagnetic dissociation cross sections[10] have been correctly extracted from the total cross sections.

Their point is that in ref.10 one assumes that the nuclear cross section scales as $\sigma_N = 2\pi(R_P + R_T)\Delta$ which is characteristic of a peripheral process concentrated in a small ring width Δ at the surface of the projectile. By adjusting the parameters of this scalling law for ^{12}C targets, where the Coulomb contribution to the total cross section is negligible, the "experimental" values of σ_N were obtained for other targets, and Coulomb contribution σ_c to the cross section were inferred by substraction. But since ^{11}Li has a long tail in its matter distribution, such procedure is doubtful. Assuming that the target is a "black disk" the nuclear striping of the outer nucleons in ^{11}Li should be

$$\sigma_N \sim 2\pi (R_P + R_T)\Delta\, P(R_T) \qquad (1)$$

where $P(R_T)$ is the probability that the outer neutrons will be removed from ^{11}Li. Due to long matter tail, this probability is not independent of R_T. Actually it shoud be approximately proportional to the area A of overlap betwen the target and the neutron halo in ^{11}Li. From simple geometrical considerations it is possible to shwo that $A_\alpha R_T$. That is, σ_N should increase like R_T^2, which has also as a consequence that "σ_c^{exp}" should be smaller than the values determined by Kobayashi et al.[10], and would come closer to the RPA calculations of Bertsch et al.[11–12] for σ_c. This is indeed a very relevant point since the electromagnetic dissociation of neutron rich nuclei reveals important aspects of their intrinsic structure.

In this paper we analysed the interplay of the nuclear and the Coulomb interaction in the reaction process

$$^{11}\text{Li} + \text{target} \rightarrow {}^{9}\text{Li} + \text{anything} \qquad (2)$$

at kinetic energies of 800 MeV/nucleon. As shown in ref.4 the nuclear Coulomb interference for the process (2) should be at most 5% of the total cross section. The, we may write the cross section as

$$\sigma = \sigma_D^{(N)} + \sigma_S^{(N)} + \sigma_C \qquad (3)$$

where $\sigma_D^{(N)}$ is the elastic (diffractive) nuclear breakup of $^{11}\text{Li} \rightarrow {}^{9}\text{Li} + (2n)$ by the target and $\sigma_S^{(N)}$ is the inelastic (stripping) cross section arising when the (2n)–system suffers an inelastic collision with the target, while ^{9}Li survives intact. σ_C is the electromagnetic dissociation (Coulomb) cross section for $^{11}\text{Li} \rightarrow {}^{9}\text{Li} + (2n)$.

Nuclear peripheral process in high energy collisions involve the calculation of eikonal phases which are dependent on the nuclear densities at the surface and on the nucleon–nucleon scattering amplitudes. For a projectile a indident on a target. A, the cross sections for peripherally induced processes are well described by adjusting the tails of the density functions so as to reproduce the correct values of the eikoal phases. This procedure results in an effective optical potential[14–15] of the form

$$U_{aA} = \langle t_{NN} \rangle \pi^{3/2} \rho_A(0)\, \rho_a(0)\, \frac{a_a^3\, a_A^3}{a^3}\, e^{-r^2/a^2} \qquad (4)$$

where the nucleon parameters are given by

$$a = \sqrt{a_a^2 + a_A^2} \quad , \qquad a_f^2 = \frac{4R_i t + t^2}{4\ell n\ 5}$$

$$R_i = 1.07\, A_i^{3/2}\ \text{fm} \quad , \qquad t = 2.4\ \text{fm} \tag{5}$$

$$\rho_i(O) = \frac{3A_i\ e^{R_i^2/a_i^2}}{8\pi\ R_i^3}\left[1 + (\pi^2\, t^2/19.36\, R_i^2)\right]^{-1} \quad .$$

There free nucleon–nucleon amplitude $<t_{NN}(E)>$ at forward direction $(\Theta = 0^o)$ can be deduced from the experiment. It can be written as

$$<t_{NN}(E)> = -\frac{E}{K}\ <\sigma_{NN}>\left[<\alpha_{NN}> + i\right]$$

where the brackets mean an isospin average of $t_{NN}(E)$ and α_{NN} over the projectile and target nucleons. For 800 MeV/nucleon, one may use[16]

$$\begin{aligned} \sigma_{pp} &= 47.3\ \text{mb} \\ \sigma_{pn} &= 37.9\ \text{mb} \\ \alpha_{pp} &= 0.06 \\ \alpha_{pn} &= -0.2 \quad . \end{aligned} \tag{6}$$

One observes that at such energy the nucleon–nucleon scattering amplitude is almost totally imaginary, meaning that the optical potential (4) is almost completely absorptive.

The transition matrix element for the elastic (diffractive) breakup in DWBA is

$$T_{fi} = \left\langle \chi^{(-)}_{\vec{k}_a}(\vec{R})\ \phi^{(-)}_{xb,f}(\vec{r}) \middle| \left[U_{xA}\left[\vec{r}_{xA}\right] + U_{bA}\left[\vec{r}_{bA}\right] - U_{aA}\left[\vec{R}_{aA}\right]\right| \chi^{(+)}_{\vec{k}_a}(\vec{R})\ \phi^{(+)}_{xb,i} \right\rangle \tag{7}$$

where ϕ_{xb} is the wavefunction for the relative motion of $x + b$ clusters (in our case $b =$ dineutron, $a = {}^{11}$Li, and $x = {}^{9}$Li), and $\chi^{(+)}_a$ is the distorted wave for a. In the final state $\chi^{(-)}_a$ represents the distorted wave in the c.m. or $x + b$. In the way (7) is written, the matrix element of U_{aA} is zero because $\left\langle \phi^{(-)}_{xb,f} \middle| \phi^{(+)}_{xb,i} \right\rangle = 0$.

We use the c.m. distorted waves

$$\chi^{(+)}_{a,i}(\vec{R}) = e^{i\vec{K}_i\cdot\vec{R}} \exp\left\{ -\frac{ik}{2E}\int_{-\infty}^{z} U_{aA}(z',b)dz' + i\phi_c(b) \right\} \tag{7.a}$$

$$\chi^{(-)*}_{a,f} = e^{-i\vec{K}_f\cdot\vec{R}} \exp\left\{ -\frac{ik}{2E}\int_{z}^{\infty} U_{aA}(z',b)dz' + i\phi_c(b) \right\} \tag{7.b}$$

where $\phi_c(b) = \frac{Z_a\ Z_A\ \alpha}{v/c}\ell n(kb)$ is the Coulomb phase, and $\alpha = 1/137$.

For the relative motion wavefunctions $\phi^{(+)}_{xb,i}$ and $\phi^{(-)}_{xb,f}$ we use simple Yukawa and plane–wave functions as in ref.3. All coordinates are referred to the lab–system, with the target origin. The coordinates $\vec{r}_{xA}$ and $\vec{r}_{bA}$ are defined by

$$\begin{aligned} \vec{r}_{xA} &= \vec{R} - \frac{m_b}{m_a}\vec{r} \\ \vec{r}_{bA} &= \vec{R} + \frac{m_x}{m_a}\vec{r} \quad . \end{aligned} \tag{8}$$

Most of the integrals involved in (7) may be calculated analytically and the details of the calculations will be shown elsewhere[17]. The breakup cross section is obtained by standard integrations over the phase–space of the fragments[17]. For $R_{^{11}Li}$ and R_{2n} we use, 5.8, 2.41 and 1.6 fm, respectively. These values are compatible with the cluster wavefunction of ^{11}Li, adjusted to reproduce the binding energy of the dineutron. The three–body calculations of ref.6 have shown that the most probable separation between these neutrons is 3.3 fm.

The "stripping" (inelastic breakup) cross section is given by[18–19]

$$\sigma_S = \frac{\sqrt{\pi}}{\Lambda}\int d^2b_x \left|S_x(b_x)\right|^2 \int d^2b_{2n} \left|\phi_{^{11}Li}(|\vec{b}_x-\vec{b}_{2n}|)\right|^2 \left[1-\left|S_{2n}(b_{2n})\right|^2\right] \qquad (8)$$

where $|S_x(b_x)|^2$ is to be interpreted as the probability that the fragment x(^{9}Li) will survive when hitting the target at an impact parameter b_x. Otherwise, $1-S_{2n}(b_{2n})^2$ is the probability that the 2n–system will suffer an inelastic collision with the target, and $d^3r_{2n}|\phi_{^{11}Li}(|\vec{b}_x-\vec{b}_{2n}|)^2$ is the probability that the 2n–system is found at distance $|\vec{b}_x-\vec{b}_{2n}|$ from ^{9}Li. The factor is in front of (8) comes from the assumption that $\phi_{^{11}Li}$ can be described by a gaussian wave–function, so that

$$\left|\phi_{^{11}Li}\right|^2 = \frac{\Lambda^3}{\pi\sqrt{\pi}} \exp\left[-\Lambda^2(z_x-z_{2n})^2\right]\cdot\exp\left[-\Lambda^2(\vec{b}_x-\vec{b}_{2n})^2\right] \quad . \qquad (9)$$

Eq.(8) was obtained after an integration over z_x and z_{2n}. The parameter Λ was chosen so that the stripping cross sectioons obtained by using (9) do not differ appreciably from what is obtained by using Yukawa–type wave–functions. The proper value of Λ was found to be given by $\Lambda = (11.2\ \text{fm})^{-1}$. This parametrization allows us to write the stripping cross section in an elegant form as

$$\sigma_S = \frac{\pi}{\Lambda^2}\sum_{j=0}^{\infty}\left[1-T_j^{(2n)}(\Lambda)\right] T_j^x(\Lambda) \qquad (10.a)$$

$$T_j^{(i)}(\Lambda) = \frac{2(\Lambda^2)^{j+1}}{j!}\int_0^{\infty} b_i^{2j+1} e^{-\Lambda^2 b_i^2} |S_i(b_i)|^2 db_i \qquad (10.b)$$

where (i = x or b).

The expression (10) is obtained by means of a series expansion of the Bessel function which results from the integration of (8) over the azimuthal angle. The factors $|S_i(b_i)|^2$ are given by

$$|S_i(b_i)|^2 = \exp\left\{-\frac{k}{E}\int_{-\infty}^{\infty}|\text{Im}\ U_i(b_i,z_i)|dz_i\right\} \qquad (11)$$

where U_i are the optical potentials for 2n + Target and ^{9}Li + Target, parametrized by eq.(4).

In addition to the nucleon fragmentation there is an important contribution from Coulomb dissociation, especially for large Z–targets. We can use the formulas obtained in ref.3 for the Coulomb dissociation of cluster nuclei, which in the limit of very low binding energy, can be written as

$$\sigma_{E1} = \frac{4\pi}{3} Z_T^2\,\alpha^2\left[\frac{c}{v}\right]^2\left[\frac{m_x Z_b - m_b Z_x}{m_a}\right]^2 \frac{1}{\eta^2}\cdot\left[\ell n\left[\frac{\gamma\hbar v}{\delta\varepsilon R}\right]-\frac{v^2}{2c^2}\right] \qquad (12.a)$$

and

$$\sigma_{E2} = \frac{\pi}{5} Z_T^2\,\alpha^2\left[\frac{c}{v}\right]^4\left[\frac{m_x^2}{m_a^2}Z_b+\frac{m_b^2}{m_a^2}Z_x\right]^2 \frac{\varepsilon^2}{\eta^4(\hbar c)^2}\cdot\left[\frac{2}{\gamma^2\xi^2}+\left[2-\frac{v^2}{c^2}\right]^2\ell n\left[\frac{1}{\delta\xi}\right]-\frac{v^4}{2c^4}\right] \quad . \qquad (12.b)$$

The total Coulomb cross section is given quite accurately by (M1 does not contribute significantly)

$$\sigma_c = \sigma_{E1} + \sigma_{E2} \quad . \tag{12.c}$$

In the above equations, $\gamma = (1-v^2/c^2)^{-1/2}$, $\delta = 0.891...$, $\varepsilon = \hbar^2\eta^2/(2\mu_{6x})$ is the binding energy of the cluster nucleus, and $\xi = \varepsilon b_{min}/(\gamma\hbar v)$. We use $b_{min} = R_{^{11}Li} + R_T$, with $R_T = 1.2\ A_T^{1/3}$ fm.

The cross section of the nuclear elastic breakup $\sigma^{(N)}_{elast}$, stripping $\sigma^{(N)}_{inel}$, electric dipole σ^{c}_{E1} and electric quadrupole σ^{c}_{E2} are given in table 1 together with the experimental data for the two–neutron removal of ^{11}Li incident on ^{12}C, ^{63}Cu and ^{208}Pb. The $\sigma^{(N)}_{elast}$ and $\sigma^{(N)}_{inel}$ for $\varepsilon = 0.2$ MeV were multiplied by a factor 1.23 in order that their sum with the Coulomb contribution would result in the experimental value for ^{12}C, which is 220 mb. The cross sections were also calculated for several other binding energies, from 0.17 MeV to 0.33 MeV.

The elastic breakup and particularly the total Coulomb cross section decreases appreciably with the binding energy, whereas the stripping cross section, having a geometrical character, does not depend on ε (if one assumes that the ^{11}Li radius is fixed).

In figure 1 we plot the nuclear contribution to the two–neutron removal cross section as compared to the experimental data. Due to the uncertainty of the binding energy of the dineutron, the calculated values lie between the two solid curves. One indeed observes that the calculated cross sections grow faster than the $A^{1/3}$–law, a result that was also obtained by G. Bertsch et al.[13] with a different method.

By choosing the binding energy of $\varepsilon = 0.2$ MeV, we find the following parametrization of σ_N with A_T

$$\sigma_N = \left[a\ A_T^{1/3} + b\ A_T^{2/3} + c\right] \text{mb} \tag{13.a}$$

with

$$a = 98{,}7 \quad , \quad b = 2.284 \quad \text{and} \quad c = -25.89 \quad . \tag{13.b}$$

For large values of A_T, the above equation results in an appreciable deviation from the $A_T^{1/3}$ scaling law[10].

The electromagnetic dissociation experimental cross sections obtained in ref. 10 are within the limits of the theoretical results, as shwon in figure 2. We observe that the scale is logarithmic and that the Coulomb cross section is strongly dependent on the binding energy of the dineutron+^{9}Li. This dependece is approximately proportional to the inverse of ε (see eq. 12a). The lower solid curve in figure 2 corresponds to $\varepsilon = 0.33$ MeV, while the upper curve corresponds to $\varepsilon = 0.17$ MeV. If the nuclear contribution to the process actually scales as in eq.(13), the experimental values of the Coulomb contribution (figure 2) should be smaller. In this case, the cluster model would not reproduce the experimental data on Coulomb dissociation, being larger by 20–30%, especially for high Z–targets.

The success of the cluster model lies on the fact that it gives the necessary amount of the electromagnetic dipole strength at low energies, so that the Coulomb dissociation cross section of ^{11}Li is rather well reproduced. The matrix elements for the photo–disintegration of ^{11}Li within the cluster model were firstly calculated in ref. 3. From their results we obtain for the electric dipole strength distribution

$$\frac{dB(E1;\uparrow)}{d(\hbar\omega)} = \frac{3\hbar^2e^2}{\pi^2\,\mu_{bx}}\left[\frac{Z_x\ m_b - Z_b\ m_x}{m_a}\right]^2 \frac{\sqrt{\varepsilon}\ (\hbar\omega - \varepsilon)^{3/2}}{(\hbar\omega)^4} \tag{14}$$

where $\mu_{bx}(\varepsilon)$ is the reduced mass (binding energy) of the cluster–system. The dipole stregth function for ^{11}Li, assuming $\varepsilon = 0.2$ MeV, has a peak at $\hbar\omega = 0.32$ MeV. This should be compared to fig. 1 of ref. 11, where the dipole response of ^{11}Li was calculated within the random phase approximation. One sees that the strong peak at very low energy

in the cluster model is completly absent in the RPA approach. In spite of the fact that the cluster–model as described here is very simplified, the above results indicate that in order to obtain the necessary amount of electric dipole strength of ^{11}Li at low energies, it is necessary to include cluster aspects in the shell model calculations, as was done in refs. 5 and 6.

From (14) we obtain that the total dipole strength in the cluster model, integrated over energy, is given by

$$B(E1) = \frac{3\hbar^2 e^2}{16\pi\, \mu_{bx}\, \varepsilon} \left[\frac{Z_x\, m_b - Z_b\, m_x}{m_a} \right]^2 \quad . \tag{15}$$

for ^{11}Li, using $\varepsilon = 0.2$ MeV, we obtain $B(E1)/e^2 = 2.25$ fm^2 in the cluster model, which is about 7% of the (non–energy–weighted) cluster sum rule for dipole excitations[20]. This means that in order to reproduce the experimental data on the Coulomb dissociation of ^{11}Li, an appreciable amount of the strength of the dipole response in ^{11}Li should be located at the ^{9}Li + 2n – channel. The Coulomb cross section is given by $\sigma_c = \int n(\omega)\sigma_\gamma(\omega)\, d\omega/\omega$, where $\sigma_\gamma(\omega)$ is the photonuclear cross section and $n(\omega)$ is a smooth function of ω (approximately a logarithm of ω). Therefore, the key information about the nuclear structure is contained in $\int \sigma_\gamma(\omega)\, d\omega/\omega$ which is directly proportional to the (non–energy weighted) integrated B(E1)–values[21,22].

The Coulomb dissociation of neutron–rich nuclei is an extremely useful tool to investigate their structure. If one could perform these measurements at Brookhaven (14.5 GeV/nucleon) and at CERN ($E_{lab} = 200$ GeV/nucleon) for example, one would obtain a Coulomb dissociation cross section of about two and three times as large as that measured by Kobayashi et al.[10]. The nulear contribution would be not so relevant, and the investigation about the nuclear structure aspects of neutron–rich nuclei would be more free of bias.

REFERENCES

1. P.G. Hansen and B. Jonson, *Europhys. Lett.* 4 (1987) 409.
2. A.B. Migdal, *Sov. J. Nucl. Phys.* **16** (1973) 238.
3. C.A. Bertulani and G. Baur, *Nucl. Phys.* **A480** (1988) 615.
4. C.A. Bertulani and M.S. Hussein, *Phys. Rev. Lett.* **64** (1990) 1099.
5. Y. Tosaka and Y. Suzuki, *Nucl. Phys.* A512 (1990) 46.
6. L. Johanssen, A.S. Jensen and P.G. Hansen, *Phys. Lett.* B, to be published.
7. C. Thibault, R. Klapisch, C. Rigaud, A.M. Poskanzer, R. Prieels, L. Lessard and W. Reisdorf, *Phys. Rev.* **C12** (1975) 644.
8. J.M. Wouters, R.H. Kraus, D.J. Vieira, G.W. Butler and K.E.G. Löbner, *Z. Phys.* **A331** (1988) 229.
9. K.H. Wilcox, R.B. Weisenmiller, G.J. Wozniak, N.A. Jelley, D. Ashery and J. Cerny, *Phys. Lett.* B59 (1975) 142.
10. T. Kobayashi et al., *Phys. Lett.* **B232** (1989) 51.
11. G. Bertsch and J. Foxwell, *Phys. Rev.* **C41** (1989) 1300, and erratum, to be published.
12. G. Bertsch, B.A. Brown and H. Sagawa, *Phys. Rev.* C39 (1989) 1154.
13. G. Bertsch, H. Esbensen and A. Sustich, *Phys. Rev.* C, to be published.
14. P.J. Karol, *Phys. Rev.* C11 (1975) 1203.
15. J.O. Rasmussen, L.F. Canto and X.T. Qiu, *Phys. Rev.* **C33** (1986) 2033.
16. L. Ray, *Phys. Rev.* C11 (1975) 1203.
17. C.A. Bertulani and M.S. Hussein, *Nulc. Phys.* A, to be published.
18. M.S. Hussein and K. McVoy, *Nulc. Phys.* A445 (1985) 124.
19. B.V. Carlson, M.S. Hussein and R. Mastroleo, IFUSP/P–822, and to be published.

20. Y. Alhassid, M. Gai and G.F. Bertsch, *Phys. Rev. Lett.* **49** (1982) 1482.

21. G. Baur, Proceedings of the International Symposium on Heavy Ion Physics and Nuclear Astrophysical Problems, Tokyo, July 21–23, 1988, World Scientific, ed. by S. Kubono , M. Ishihara and T. Nomura, p.225.

22. G. Baur and C.A. Bertulani, *Nucl. Phys.* **A482** (1988) 313c.

TABLE CAPTION

1. The elastic (σ_N^{elast}), inelastic (σ_N^{inel}), nuclear $\left[\sigma_N = \sigma_N^{elast} + \sigma_N^{inel}\right]$, electric dipole ($\sigma_{E1}$), electric quadrupole ($\sigma_{E2}$), Coulomb $\left[\sigma_c = \sigma_{E1} + \sigma_{E2}\right]$, nuclear experimental ($\sigma_N^{exp}$), and Coulomb experimental (σ_c^{exp}) cross sections for the dissociation of ^{11}Li (0.8 GeV/Nucleon) projectiles incident on several targets, as a function of the binding energy of the ^{9}Li + dineutron system.

FIGURE CAPTIONS

Figure 1. Two–neutron removal cross sections of ^{11}Li (0.8 GeV/nucleon) projectiles due to the nuclear interaction with the targets, as a function of the target number. Due to the uncertainty of the binding energy of ^{11}Li, the theoretical results lie between the two solid curves. The experimental data of ref. 10 are also shown.

Figure 2. Same as figure 1, but for the electromagnetic dissociation of ^{11}Li.

TABLE I

^{11}Li + X → ^{9}Li + anything

σ(mb)

^{11}Li + ^{12}C

ε	σ^{N}_{elast}	σ^{N}_{inel}	σ_N	σ_{E1}	σ_{E2}	σ_c	σ_N^{exp}	σ_c^{exp}
0.17	79	136	215	9.1	0.5	9.6		
0.2	76	136	212	7.6	0.4	8.0	220	0
0.25	73	136	209	5.9	0.3	6.2	±10	
0.3	70	136	206	4.8	0.2	5.0		
0.33	69	136	205	4.3	0.2	4.5		

^{11}Li + ^{63}Cu

ε	σ^{N}_{elast}	σ^{N}_{inel}	σ_N	σ_{E1}	σ_{E2}	σ_c	σ_N^{exp}	σ_c^{exp}
0.17	187	223	410	203	8	211		
0.2	180	223	403	169	6	175	320	210
0.25	170	223	393	131	5	136	±20	±40
0.3	162	223	385	105	4	109		
0.33	158	223	381	94	3	97		

^{11}Li + ^{208}Pb

ε	σ^{N}_{elast}	σ^{N}_{inel}	σ_N	σ_{E1}	σ_{E2}	σ_c	σ_N^{exp}	σ_c^{exp}
0.17	339	315	654	1565	43	1608		
0.2	324	315	639	1295	33	3128	420	890
0.25	304	315	619	996	24	1020	±30	±100
0.3	289	315	604	803	17	820		
0.33	281	315	596	717	15	732		

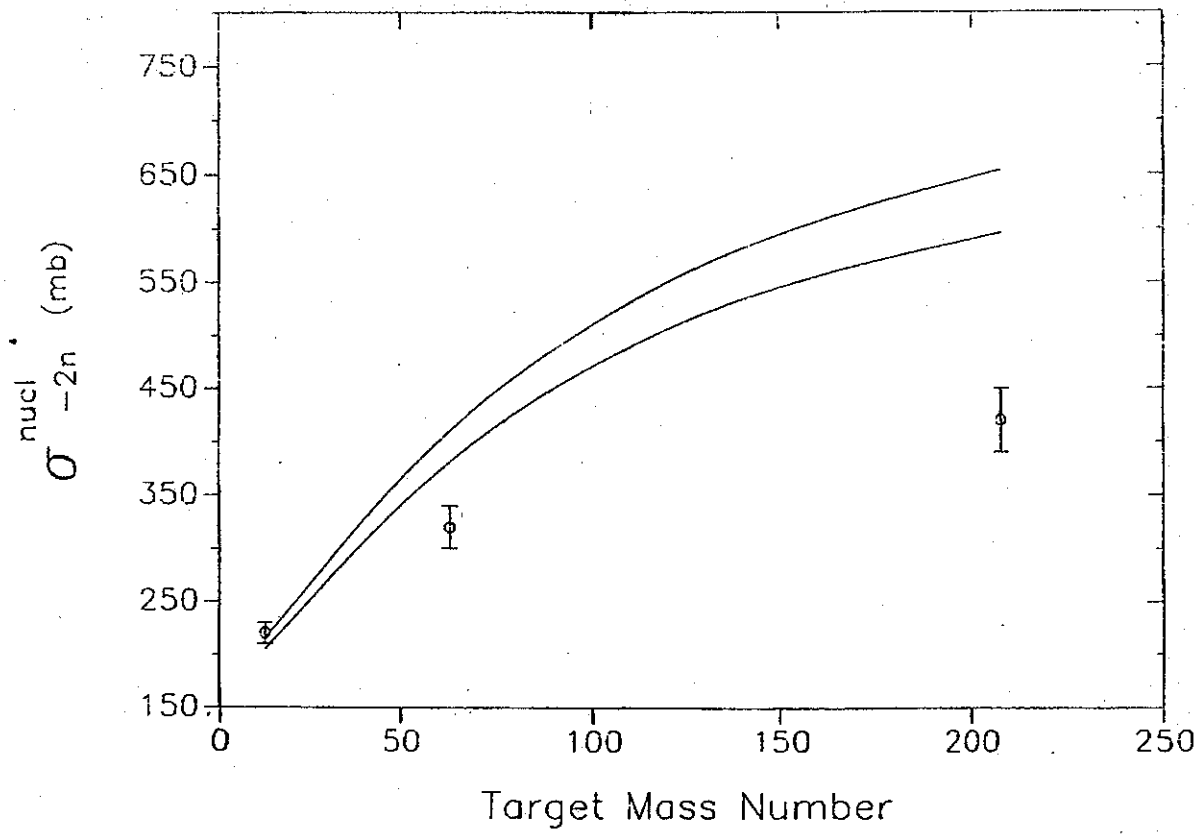
750
650
550
450
350
250
150
0
50
100
150
200
250
σ^{nucl}_{-2n} (mb)
Target Mass Number

Fig. 1

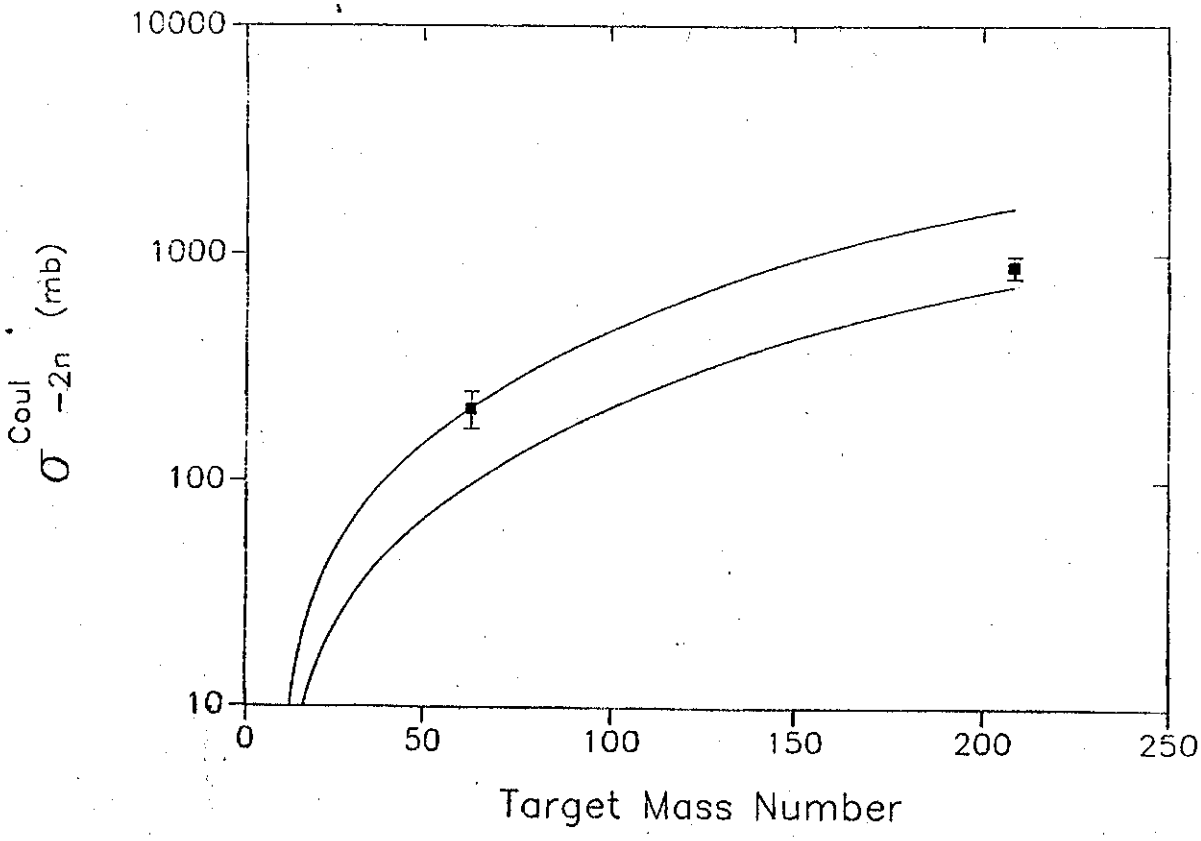
10000
1000
100
10
0
50
100
150
200
250
σ^{Coul}_{-2n} (mb)
Target Mass Number

Fig. 2